Non-destructive readout of 2D and 3D dose distributions using a disk-type radiophotoluminescent glass plate

doi: 10.1088/1757-899X/80/1/012001

Non-destructive readout of 2D and 3D dose distributions using a disk-type radiophotoluminescent glass plate

2015 IOP Conf. Ser.: Mater. Sci. Eng. 80 012001

(http://iopscience.iop.org/1757-899X/80/1/012001)

IOP Conf. Series: Materials Science and Engineering **80** (2015) 012001 doi:10.1088/1757-899X/80/1/012001

Non-destructive readout of 2D and 3D dose distributions using a disk-type radiophotoluminescent glass plate

T Kurobori[1], Y Maruyama[1, 2], Y Miyamoto[3], T Sasaki[1] and H Nanto[4]

[1] Graduate School of Natural Science and Technology, Kanazawa University, Kakuma, Kanazawa 920-1192, Japan
[2] Pulstec Industrial Corporation, 7000-35 Nakagawa, Hosoe, Kita-ku, Hamamatsu 431-1304, Japan
[3] Oarai Research Center, Chiyoda Technol Corporation, 3681 Narita-cho, Oaraimachi, Ibaraki 311-1313, Japan
[4] Adv. Mater. Sci. R&D Center, Kanazawa Institute of Technology, 3-1 Yatsukaho, Hakusan 924-0838, Japan

E-mail: kurobori@staff.kanazawa-u.ac.jp

Abstract. Novel disk-type X-ray two- and three-dimensional (2D, 3D) dose distributions have been developed using atomic-scale defects as minimum luminescent units, such as radiation-induced silver (Ag)-related species in a Ag-activated phosphate glass. This luminescent detector is based on the radiophotoluminescence (RPL) phenomenon. Accurate accumulated dose distributions with a high spatial resolution on the order of microns over large areas, a wide dynamic range covering three orders of magnitude and a non-destructive readout were successfully demonstrated for the first time by using a disk-type glass plate with a 100-mm diameter and a 1-mm thickness. In addition, the combination of a confocal optical detection system with a transparent glass detector enables 3D reconstruction by piling up each dose image at different depths within the material.

1. Introduction

The passive dosimeters based on the radiophotoluminescence (RPL) [1-3], optically stimulated luminescence (OSL) [4, 5], photoluminescence (PL) [6-8] and thermoluminescence (TL) [9] phenomena have been widely used for personal, environmental and clinical dosimetry. Although the four types of passive luminescent dosimeters each have advantages and disadvantages [9-11], few reports for 2D and 3D dose distributions on large areas have been published. A dosimeter made of silver (Ag)-activated phosphate glass, which is known as the most common RPL material, has been recognized as possessing several desirable characteristics, such as non-destructive readout capabilities, long-term stability against fading, wide dynamic range and uniformity/batch homogeneity [12].

Recently, a novel disk-type 2D imaging detector with the aforementioned superior characteristics of the RPL dosimeter (referred to as “the glass batch”) was proposed and demonstrated [13] for the first time. The 2D dose distribution written in the form of atomic-scale luminescent defects by X-ray irradiation was rapidly reconstructed with a high spatial resolution of 1 μm and a sensitivity of 1 mGy, when the disk-type detector with a diameter of 80 mm was rotated at a rate of 400 rpm (6.7 Hz) to read out the accumulated dose information.

In addition, a comparative study of 2D dose images from Ag-activated phosphate glass using the Ag^{2+} colour centres (CCs) and LiF thin films using F-aggregate CCs based on the RPL and PL phenomena was performed, respectively, and their performances were also evaluated [14]. The 2D dose images with a wide dynamic range covering eight orders of magnitude were successfully demonstrated by combining a Ag-doped glass detector with a LiF thin film detector deposited on a glass substrate. These disk-type detectors were rotated at a rate of 2400 rpm (40 Hz). A detailed description of the optical and dosimetric properties of Ag-related defects in Ag-activated phosphate glass has been published elsewhere [15, 16].

In this paper, first, the optical properties of X-ray-irradiated Ag-activated phosphate glass were studied under absorbed doses from 0.1 to 10 Gy. Specifically, the effects of the absorption rate at an exciting wavelength of 371 nm and the re-absorption rate at an emitting wavelength of 630 nm (i.e., orange RPL) were evaluated from the optical absorption spectra. Second, an accurate 2D dose distribution with a high spatial resolution, wide dynamic range and non-destructive readout was successfully demonstrated using a disk-type Ag-activated phosphate glass plate. Finally, the use of a confocal detection system and a transparent glass detector allows one to reconstruct a 3D dose distribution by combining each image at different depths from the vicinity of the surface to ≈400 μm.

2. Experimental procedure

A commercially available Ag-activated phosphate glass was used as 2D and 3D RPL detectors. Although the weight composition of the used detector was the same as that of the FD-7 (Asahi Techno Glass), i.e., 31.55% P, 51.16% O, 6.12% Al, 11.00% Na and 0.17% Ag, the size and shape were different; the detector was a disk-type plate with a diameter of 100 mm and a thickness of 1 mm.

In this work, the samples were coloured by irradiation from an X-ray unit (8.05 keV) with a copper target operating at 30 kV and 20 mA. The absorbed doses on the samples ranged from 0.1 to 10 Gy. The dose rate from the X-ray unit was calibrated with a commercially available Ag-activated phosphate glass dosimeter. The irradiation dose measurements were performed with a technique based on a combination of a pulsed UV laser excitation and a photon counting system at the Oarai Research Centre of the Chiyoda Technol Corporation, resulting in a dose rate of 117 mGy/min at a distance of 320 mm from the X-ray tube.

Optical absorption (OA) was obtained at room temperature (RT) using a Hitachi U-3900H UV-VIS. The RPL spectra were obtained by a Hitachi F-2500 fluorescence spectrophotometer. For all of the optical measurements, the samples were cut to a suitable size from the original glass dosimeter plate in approximately $10 \times 7 \times 1\text{-mm}^3$ rectangular plates. The radiative lifetime measurements of the blue and orange RPL were performed using a fluorescence lifetime spectrometer (Quantaurus-Tau C11367-14, Hamamatsu Photonics) at RT. Light that was 340 nm from an LED source was used as an excitation beam. The total time resolution was less than 1.0 ns.

3. Results and discussion

Figures 1(a) and (b) show the OA and RPL spectra in Ag-activated phosphate glass with a thickness of 1 mm, respectively, before and after X-ray irradiation under absorbed doses from 0.1 to 10 Gy. Each Ag-activated glass plate was heated to 100 ºC for 15 min to suppress the "build-up" kinetics after X-ray irradiation. A set of absorption spectra were attributed to the superposition of a number of individual absorption bands corresponding to the atomic Ag atoms, charged Ag-aggregate CCs and neutral Ag molecular clusters and phosphorous- and oxygen-related species in the range from 250 to 700 nm, as already reported [15, 16]. The primary band peaking at 310 nm emits the orange RPL at 560 nm, which is attributed to the Ag^{2+} centres. Another band peaking at 340 nm emits the blue RPL at 450 nm, which is attributed to the Ag^0 centres. In this work, the blue and orange RPL were simultaneously emitted by an excitation wavelength at 371 nm because of the superposition of the blue and orange absorption bands. Note that both peak bands for the blue and orange RPL were shifted to the longer wavelengths from 450 to 470 nm and from 560 to 630 nm, respectively, by a UV laser excitation. In addition, the dosimetric

relationship between the response of the blue and orange RPL intensity and X-ray absorbed doses from 0.1 to 10 Gy exhibited a good dose linearity response. From Fig. 1(a), we estimated the values of the absorption coefficient and re-absorption rate when light at 630 nm propagates a 500-μm length in the X-ray-irradiated glass under an absorbed dose of 1 Gy. The values are 1.15×10^{-5} (μm^{-1}) and 0.57 %, respectively. For an excitation wavelength at 371 nm, the corresponding values are 1.28×10^{-4} (μm^{-1}) and 6.2 %, respectively. To acquire accurate 3D dose distributions, one must take these values into consideration.

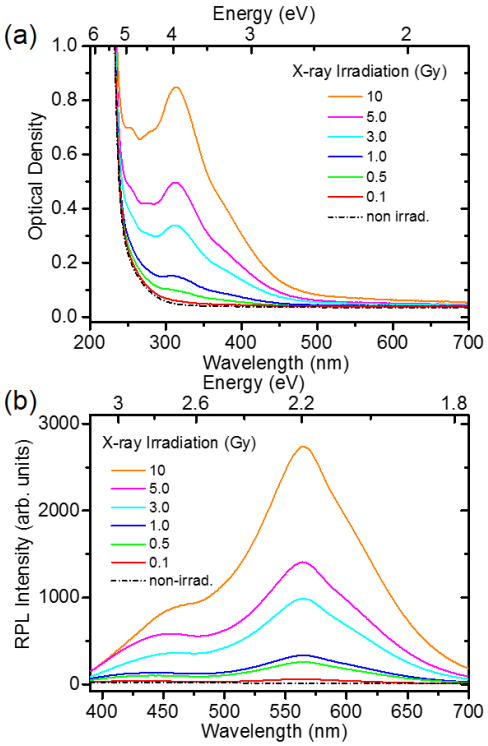

Figure 1. (a) OA spectra of Ag-activated phosphate glass with a thickness of 1 mm before and after X-ray irradiation with absorbed doses from 0.1 to 10 Gy. (b) Corresponding RPL spectra excited at 340 nm before and after X-ray irradiation at RT.

A schematic view of the experimental arrangement employed to measure the 2D and 3D dose distributions is shown in Fig. 2. Collimated light at 371 nm from a cw laser diode (LuxX 371-70, Omicron GmbH) with a maximum power of 70 mW was used as an excitation source. For reading, a low-level power between 10 and 20 mW was used for stimulating the orange RPL at 630 nm. The laser beam was expanded and reflected with a dichroic beam splitter (B/S) (#86-330, Edmund Optics) and focused in the vicinity of the surface for the disk-type detector by a Nikon LU Plan Fluor objective lens (100×, NA=0.90) while reading out the image. The objective lens was simultaneously used for both laser excitation and emission collection. Each detector was attached to a spindle on a linear translation stage, which was rotated at a rate of 2400 rpm and controlled to translate the laser beam spot from the outer disk to the inner disk in the radial direction with a pitch of 20 μm. Additional optical filters, including band-pass (BP)(#86-736, 375±5 nm, Edmund Optics), long-pass (LP) (#62-981, Edmund Optics), BP for the orange RPL (#84-797, 600±25 nm, Edmund Optics) and BP for the blue RPL (#86-962, 475±25 nm, Edmund Optics), were inserted to reject the reflected emission and residual stimulating laser light, respectively. Only the signal was detected by the photomultiplier tube (PMT) (#H10720-20, Hamamatsu Photonics), which then digitized the signal using a 500-kSamples/s, 16-bit analogue-to-digital (A/D) converter. The dose distribution was reconstructed by a personal computer. The total readout and reconstructed times were one to five min, depending on the track pitch (10 to 100 μm) and the number of tracks. The glass detector was irradiated with absorbed doses from 1 to 3 Gy. After X-ray irradiation, the RPL detector was preheated at 100 ºC for 15 min before measuring.

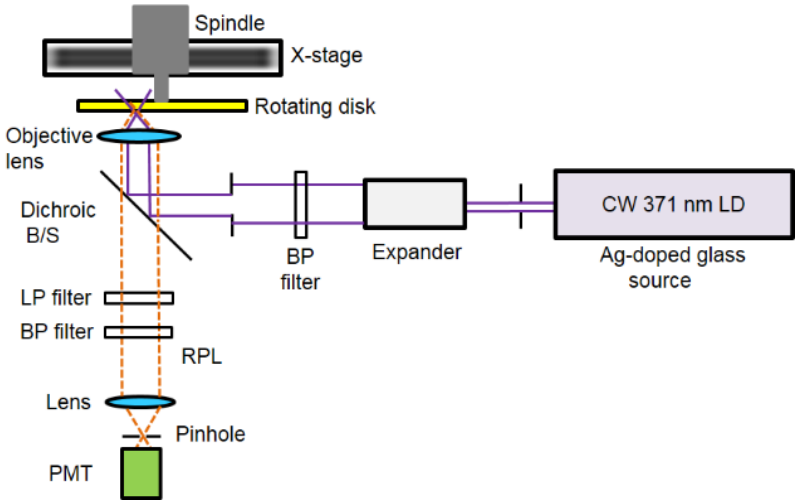

Figure 2. Schematic diagram of a disk-type RPL glass detector and a confocal optical detection system.

To investigate the dependence of the RPL intensity on the radius of the disk and on the radiative lifetime of the orange and blue RPL, a line pattern (orange coloured area) was drawn on the surface of the detector as shown in Fig. 3(a). The width of the line written by X-rays was approximately 7 mm. Figure 3(b) shows the waveform displayed as a function of the radius, i.e., r=45, 30, 20, 10, 5 and 2 mm, as rotating at a speed of 2400 rpm (period=25 ms) and also shows the corresponding length per division on an oscilloscope. Figure 3(b) also shows the reconstructed dose image of the irradiated line.

As shown in Fig. 3 (b), the spatial resolution of the inner disk becomes higher than that of the outer disk. In this work, each revolution of the disk is divided into 12,500 pixels; therefore, the minimum pixel size can be estimated as 25 μm at r=50 mm and as 3.7 μm at r=7.5 mm. In addition, the transit time of the luminescence, moving across the spot size with nearly 1 μm in diameter focused by an objective lens (100×), can be estimated as 80 ns at r=50 mm and as 530 ns at r=7.5 mm. Therefore, the RPL intensity depends strongly on the radiative lifetime of the detector when the revolutions of the disk are constant (in this work, 2400 rpm).

For the lifetime of the RPL, the following experiments were performed: the decay curves of the blue and orange RPL for X-ray-irradiated glass were taken at RT. The lifetime value of the blue RPL was considerably shorter than that of the orange RPL. In addition, the lifetime values depend on the absorbed doses, when increasing the doses from 0.1 to 10 Gy, and the blue and orange RPL values decrease from 4.7 to 4.3 ns and from 2400 to 2200 ns, respectively. As a result, in the case of the blue RPL, the RPL intensity depends strongly on the lifetime (4.5 ns under a dose of 1Gy) because the intensity decreases remarkably at the inner disk.

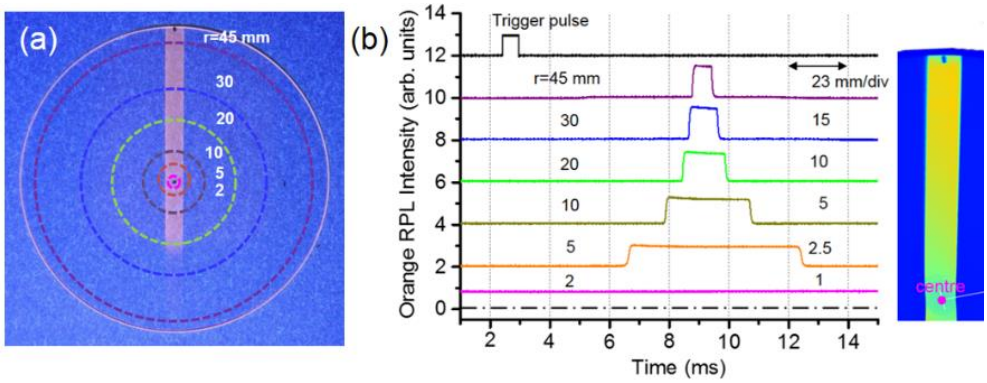

Figure 3. (a) A line pattern with a width of 7 mm drawn on the surface by X-rays. (b) Waveform of the orange RPL intensity as a function of the radius at various positions and the reconstructed 2D image (right).

Figure 4 (a) shows a photo image (“Hassam House" in Kobe) of the mask used for X-ray irradiation. Figures 4 (b) and (c) show a set of reconstructed dose distributions obtained from the disk-type Ag-activated phosphate glass based on the orange and blue RPL, respectively, with an absorbed dose of 3 Gy. The full-scale input voltage of an A/D converter was set between 0 and 2.5 V with a resolution of 16 bit. The reconstructed images indicate the red regions of the colour axes corresponding to higher concentration levels, while the blue regions indicate areas in which soft X-rays could not pass through the 250-μm-thick stainless steel attached to the detector as a mask or as non-exposure parts during X-ray irradiation. Figure 4 (d) shows an enlargement map of the parts in Fig. 4 (b). In the case of the RPL detector, steep gradients of dose distribution levels are clearly resolved with the highest image contrast. Changing the full-scale input voltage after acquiring a reconstructed 2D image, lower level distributions can be observed as low as several mGy.

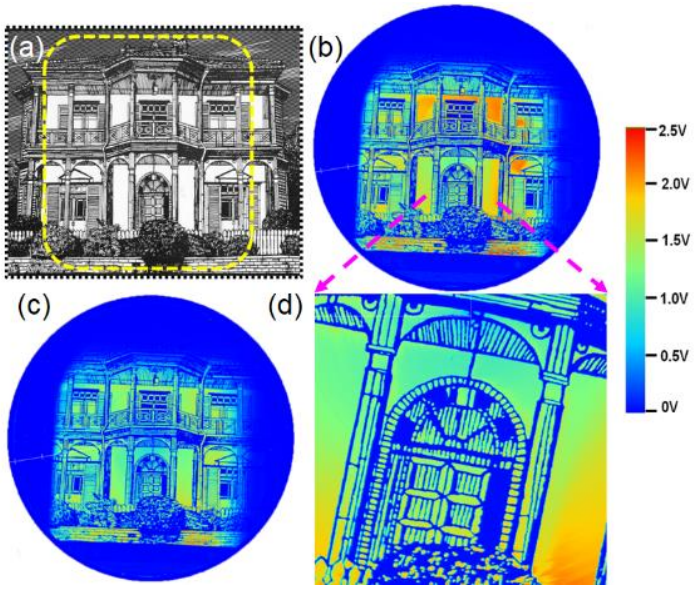

Figure 4. (a) Photo image of the mask used for X-ray irradiation. A set of reconstructed dose distributions acquired using the (b) orange and (c) blue RPL, respectively, and (d) an enlargement image of (b).

Figure 5 shows a series of the 2D reconstructed dose distributions obtained from the disk-type Ag-activated glass detector with a dose value of 3 Gy. The use of a confocal detection system and a 0.90 NA objective lens having a working distance of 1 mm enables one to reconstruct 3D dose distributions within the transparent detector by combining area images at different depths, i.e., the vicinity of the surface, 100, 200, 300 and 400 μm below the surface.

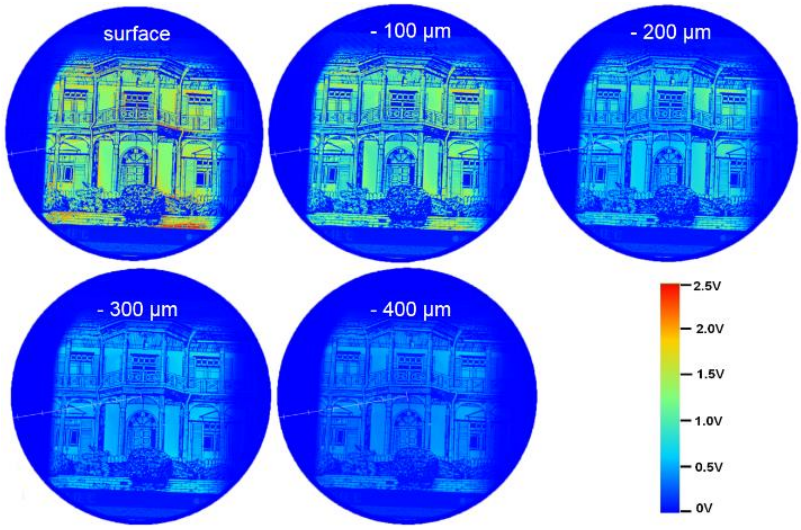

Figure 5. Reconstructed dose distributions acquired for each image at different depths of 0, 100, 200, 300 and 400 μm below the surface.

4. Conclusion

The data obtained in this study led to the following conclusions: (1) The capabilities of the reconstructed 2D dose images based on the orange and blue RPL in a disk-type Ag-activated phosphate glass with a high spatial resolution on the order of microns, a wide dynamic range covering three orders of magnitude and a non-destructive readout were successfully demonstrated. (2) The spatial resolution and RPL intensity of a disk-type detector depend strongly on the radius of the disk and the lifetime values of the material, respectively. (3) The use of a confocal detection system and the high luminescent RPL glass allow one to reconstruct a 3D image by combining each image at different depths from the surface to ≈400 μm.

Three processes, including preheating, reading and erasing, which are necessary during the use of the detector, can be performed with only a UV laser by adjusting the stepwise output levels and are currently underway. In addition, the use of the blue RPL allows measurements of the high-speed revolutions of the disk. This detector should be suitable for microradiography, X-ray microscopy, radiation diagnostics and fluorescent nuclear track applications.

Acknowledgements

T. K would like to thank Mr. Y. Koguchi and Mr. N. Takeuchi at Chiyoda Technol Corporation for their contributions to the sample preparation. This work was supported by JSPS, Grand-in-Aid for Scientific Research (B), No.26289362.

References

[1] Yamamoto T, Maki D, Sato F, Miyamoto Y, Nanto H and Iida T 2011 *Radiat. Meas.* ***46*** *1554.*
[2] Yokota R and Imagawa R 1966 *J. Phys. Soc. Jpn.* ***23*** *1038*.
[3] Perry J A 1987 *Radiophotoluminescence in Health Physics (Adam Hilger) New York.*
[4] Yukihara E G and McKeever S W S 2011 *Optically Stimulated Luminescence (John Wiley & Sons) New York*.
[5] Akselrod G M, Akselrod M S, Benton E R and Yasuda N 2006 *Nucl. Instr. and Meth. B* ***247*** *295.*
[6] Baldacchini G, Bonfigli F, Faenov A, Flora F, Montereali R M, Pace A, Pikuz T, Reale L 2003 *J. Nanosci. Nanotech.* ***3*** *483.*
[7] Montereali R M, Almaviva S, Bonfigli F, Cricenti A, Faenov A, Flora F, Caudio P, Lai A, Martellucci S, Nichelatti E, Pikuz T, Reale L, Richetta M, Vincenti M A 2010 *Nucl. Instrum. Methods Phys. Res. Sect. A* ***623*** *758*.
[8] Kurobori T, Miyamoto Y, Maruyama Y, Yamamoto T and Sasaki T 2014 *Nucl Instrum. Methods Phys. Res. Sect. B* ***326*** *76.*
[9] Olko P 2010 *Radiat. Meas.* ***45*** *506*.
[10] Garcier Y, Cordier G, Pauron C and Fazileabasse J 2007 *Radiat. Prot. Dosim.* ***124*** *107*.
[11] Knežević Ž, Stolarczyk L, Bessieres I, Bordy J M, Miljannić S and Olko P 2013 *Radiat. Meas.* ***57*** *9*.
[12] T Hsu S -M, Yeh S -H, Lin M -S and Chen W -L 2006 *Radiat. Prot. Dosim.* ***119*** *327*.
[13] Kurobori T and Nakamura S 2012 *Radiat. Meas.* ***47*** *1009.*
[14] Kurobori T and Matoba A 2014 *Jpn. J. Appl. Phys.* ***53*** *02BD14*.
[15] Kurobori T, Zheng W, Miyamoto Y, Nanto H and Yamamoto T 2010 *Opt. Mater.* ***32*** *1231*.
[16] Zheng W and Kurobori T 2011 *J. Lumin.* ***131*** *36*.